NANO LETTERS

2008
Vol. 8, No. 8
2442-2446

Macroscopic Graphene Membranes and Their Extraordinary Stiffness

Tim J. Booth,*,† Peter Blake,‡ Rahul R. Nair,† Da Jiang,‡ Ernie W. Hill,§ Ursel Bangert,¶ Andrew Bleloch,|| Mhairi Gass,|| Kostya S. Novoselov,† M. I. Katsnelson,⊥ and A. K. Geim†

Department of Physics and Astronomy, Schuster Laboratory, Manchester University, Brunswick Street, Manchester M13 9PL, United Kingdom, Graphene Industries Ltd, 32 Holden Avenue, Manchester M16 8TA, United Kingdom, Center for Mesoscience and Nanotechnology, Manchester University, Oxford Road, Manchester M13 9PL, Materials Science Center, Manchester University, Grosvenor Street, Manchester M1 7HS, United Kingdom, SuperSTEM, Daresbury Laboratory, Daresbury, Cheshire WA4 4AD, United Kingdom, and Institute for Molecules and Materials, Radboud University Nijmegen, 6525 AJ, Nijmegen, The Netherlands

Received May 16, 2008; Revised Manuscript Received June 5, 2008

ABSTRACT

The properties of suspended graphene are currently attracting enormous interest, but the small size of available samples and the difficulties in making them severely restrict the number of experimental techniques that can be used to study the optical, mechanical, electronic, thermal, and other characteristics of this one-atom-thick material. Here, we describe a new and highly reliable approach for making graphene membranes of a macroscopic size (currently up to 100 μm in diameter) and their characterization by transmission electron microscopy. In particular, we have found that long graphene beams supported by only one side do not scroll or fold, in striking contrast to the current perception of graphene as a supple thin fabric, but demonstrate sufficient stiffness to support extremely large loads, millions of times exceeding their own weight, in agreement with the presented theory. Our work opens many avenues for studying suspended graphene and using it in various micromechanical systems and electron microscopy.

Graphene is a one-atom-thick crystal consisting of carbon atoms that are sp^2 bonded into a honeycomb lattice. Its exceptional properties continue to attract massive interest, making graphene currently one of the hottest topics in materials science.[1] Much experimental work has so far been carried out on graphene flakes produced on top of oxidized silicon wafers by micromechanical cleavage.[2–4] More recently, procedures were developed to process graphene crystallites further and obtain suspended (free-standing) graphene,[5–10] which provided valuable information about its microscale properties such as long-range crystal order and inherent rippling.[8] Graphene membranes with lateral dimensions of the order of 0.1−1 μm were previously fabricated either by etching a substrate material away from beneath a graphene crystallite, which left it supported by a gold "scaffold" structure,[5] by direct transfer of graphene crystals onto an amorphous carbon film,[7] or by cleavage on silicon wafers with etched trenches.[6,9,10] The small sample size, especially for the case of suspended graphene, remains a major limiting factor in various studies and precludes many otherwise feasible experiments. In this communication, we report a technique for making large graphene membranes with sizes that are limited only by the size of initial flakes obtained by micromechanical cleavage, currently up to 100 μm diameter. These membranes can be produced reliably from chosen crystallites with a typical yield of more than 50%. The final samples are mechanically robust, easy to handle, and compatible with the standard holders for transmission electron microscopy (TEM), which allows the use of graphene as an ultimately thin and nonobstructing support in electron diffraction or high-resolution transmission electron microscopy studies (see Figure 1). Furthermore, our procedures do not involve any aggressive etchants that can lead to the "oxidation" of graphene[11] and/or its irreversible contamination, which makes the technique suitable for incorporation into complex microfabrication pathways. The membranes demonstrated here should facilitate further studies of mechanical, structural, thermal, electrical, and optical

* Author to whom correspondence should be addressed. E-mail: tim.j.booth@gmail.com.
† Schuster Laboratory, Manchester University.
‡ Graphene Industries Ltd.
§ Center for Mesoscience and Nanotechnology, Manchester University.
¶ Materials Science Center, Manchester University.
|| Daresbury Laboratory.
⊥ Radboud University Nijmegen.

10.1021/nl801412y CCC: $40.75
Published on Web 07/02/2008

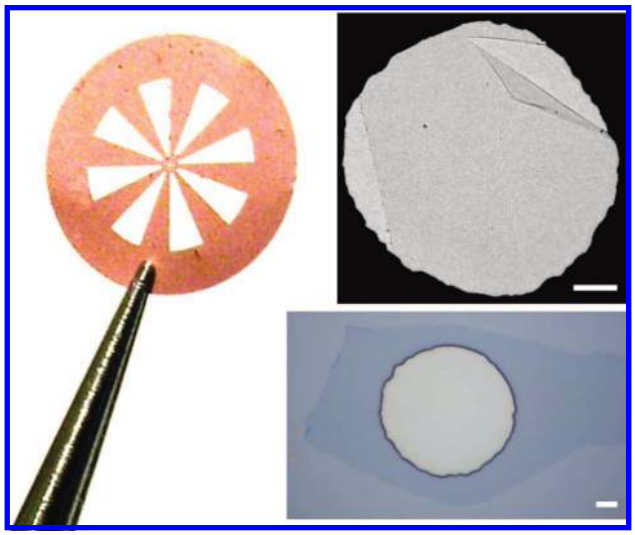

Figure 1. Graphene membranes. Left: Photograph of a standard support grid for TEM (3 mm in diameter) with a central aperture of 50 μm diameter covered by graphene. Bottom: Optical image of a large graphene crystal covered by photoresist in the place where the aperture is planned. Top: TEM micrograph of one of our graphene membranes that was partially broken during processing, which made graphene visible in TEM. Scale bars: 5 μm.

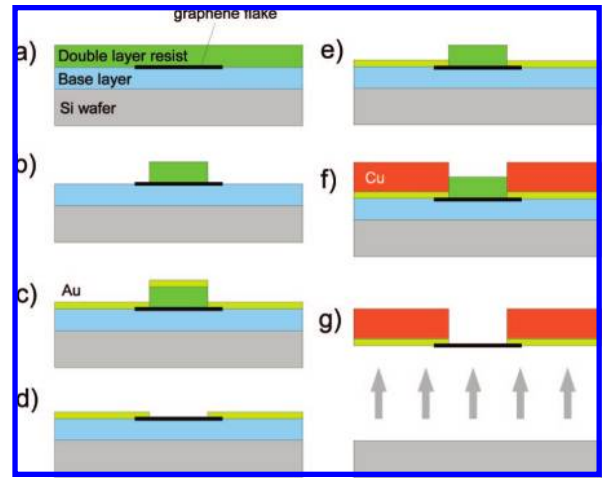

Figure 2. Microfabrication steps used in the production of graphene membranes.

properties of this new material because graphene samples can now be used in a much wider range of experimental systems. We have also found that graphene does not meet the current perception of these one-atom-thick films as being extremely fragile and prone to folding and scrolling.[12,13] In fact, graphene appears to be so stiff and robust that crystallites supported by one side can freely extend 10 μm away from a scaffold structure. The latter observation is explained within elasticity theory by a huge Young's modulus of graphene.

Figure 1 shows examples of our final samples whereas Figure 2 explains the fabrication steps involved. Graphene crystals are first prepared by standard micromechanical cleavage techniques.[3] Sufficiently large flakes produced in this way are widely distributed over a substrate (occurring with a typical number density of <1 per cm^2) and in a great minority as compared with thicker flakes. This prevents their identification via atomic-resolution techniques such as scanning probe or electron microscopies because of either prohibitively small search areas or a lack of response specific to single-layer graphene.[3] Fortunately, one-atom-thick crystals can still be identified on surfaces covered with thin dielectric films because of a color shift induced by graphene, which allows crystals to be found rapidly with a trained eye and a quality optical microscope.[14] In the current work, we have used Si wafers that, in contrast to the standard approach,[2–4] are not oxidized but instead covered with a 90 nm thick film of polymethyl methacrylate (PMMA) (referred to as a base layer in Figure 2a). The optical properties of PMMA are close to those of SiO_2, and the visible contrast of graphene is optimal at this particular thickness.[14] The PMMA film also serves later as a sacrificial layer during the final liftoff (see below).

Once a suitable graphene crystal is identified in an optical microscope, we employ photolithography to produce a chosen pattern (in our case, a TEM grid) on top of graphene (we usually used a double-layer resist consisting of 200 nm polymethyl glutarimide (PMGI) from MicroChem Corp and 200 nm S1805 from Rohm and Haas; Figure 2a,b). A 100 nm Au film with a 5 nm Cr adhesion layer is thermally evaporated after developing the resist (Figure 2c). Liftoff of the metal film is not performed in acetone, which would destroy the base layer, but in a 2.45 wt % TMAH solution (MF-319 developer; MicroChem) at 70 °C, resulting in a minimal etch rate for PMMA (<5 Å min^{-1};[15] Figure 2d).

The next step involves another round of photolithography (Figure 2e) in which the graphene crystal is remasked with the same photoresist. The mask serves here to protect graphene during electrodeposition, when a thick copper film is electrochemically grown on top of the Au film, repeating the designed pattern (Figure 2f). We have chosen a $CuSO_4$/H_2SO_4 electrolyte because of its low toxicity, resist and substrate compatibility, and ease of deposition. Finally, acetone is used to strip the remaining resist, releasing the copper TEM grid with the attached graphene membrane (Figure 2g). The sample is dried in a critical point dryer to prevent the membrane rupturing due to surface tension. A copper thickness of 10−15 μm is found to be sufficiently robust for reliable handling of the samples. The resulting membranes are then ready for transmission electron microscopy and other graphene studies.[16]

Figure 3 shows an atomic-resolution TEM image of one of our membranes. The crystal lattice of graphene is readily visible in the clean central area of the micrograph, which is surrounded by regions with hydrocarbon contamination. In the clean region, one can also notice a number of defects induced by electron-beam exposure (100 keV). Note that, prior to TEM studies, our membranes were annealed in a hydrogen atmosphere at 250 °C, which allowed the removal of contaminants such as, for example, resist residues.[17] Nevertheless, graphene is extremely lipophilic, and we find that a thin contamination layer is rapidly adsorbed on membranes after their exposure to air or a TEM vacuum.

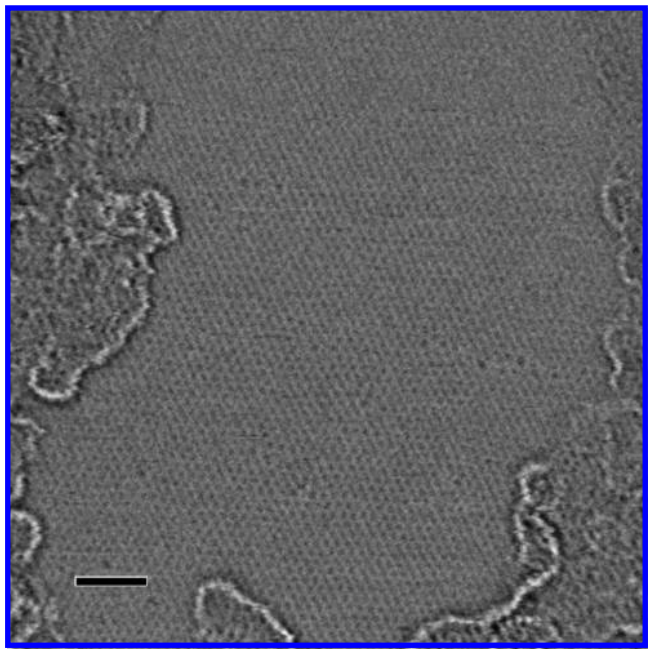

Figure 3. High resolution bright field micrograph of single-layer graphene. The image was taken at 100 keV with the Daresbury SuperSTEM fitted with a Nion spherical aberration corrector. Contamination is visible at the edges of the field. Several dark spots seen within the clean central area are the beam-induced knock-on damage that becomes increasingly more pronounced for extended exposures. Scale bar: 2 nm.

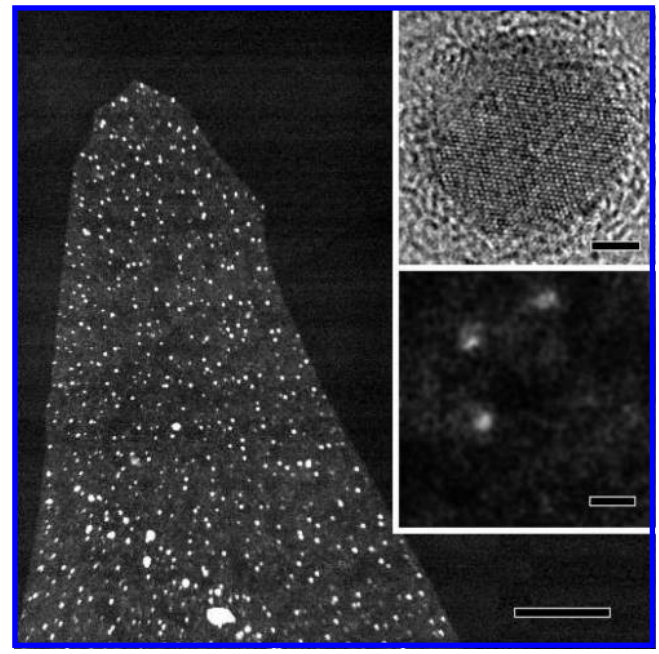

Figure 4. HAADF micrograph of a section of a graphene membrane that fractured during annealing. The graphene crystal is supported from one side only. White dots are copper nanoparticles. Scale bar: 1 μm. Top inset: high resolution bright field STEM micrograph of such a Cu particle (Ø 8.0 nm; scale bar: 2 nm). Low inset: HAADF image of individual atoms on graphene; scale bar: 2 Å.

Annealing the samples at temperatures higher than 300 °C is found to trigger redeposition of copper and the formation of nanoparticles on the surface of graphene (Figure 4). These particles are useful as a source of high contrast to aid focusing in TEM, and as the in situ calibration standard based on a copper lattice constant. The top inset of Figure 4 shows one such Cu crystal. Furthermore, we have used the high angle annular dark field (HAADF) mode of the SuperSTEM, which is very sensitive to chemical contrast. Three foreign atoms found within one small area of a graphene membrane are clearly seen on the HAADF image as white blurred spots (lower inset of Figure 4) and can be ascribed to adsorbed oxygen or hydroxyl molecules. This illustrates that graphene membranes can be used as an ideal support for atomically resolved TEM studies. Indeed, being one-atom-thick, monocrystalline, and highly conductive, graphene produces a very low background signal. Diffraction spots due to graphene can be isolated and minimally obscure diffraction patterns of investigated samples placed on such membranes. For spectroscopic applications including X-ray microanalysis, graphene also provides a minimal background due to the low atomic number and a low concentration of impurities adsorbed on graphene's surface.

One of the most unexpected and counter-intuitive results of our work is the observation of graphene crystallites supported from only one side. Figure 4 shows such a crystal left after a membrane was fragmented during its annealing (probably because of thermal stress). In this case, the graphene sliver extends nearly 10 μm from the metal grid, in the absence of any external support. This contradicts the perception that graphene is extremely supple and should curl or scroll to minimize the excess energy due to free surface energy and dangling bonds.[12,13] The previous observations[5–7] on suspended graphene seemed to be in agreement with the latter assumption showing scrolled edges.[5] Figure 4 proves that, on the contrary, graphene is exceptionally stiff. We believe that the fundamental difference between the case of Figure 4 and the earlier observations is that our crystals were fragmented in a gas atmosphere rather than in liquid (our membranes broken in a liquid were also strongly scrolled and folded).

To appreciate the stiffness of graphene, we note that the effective thickness a of single-layer graphene from the point of view of elasticity theory[18] can be estimated as $a = \sqrt{\kappa/E} \approx 0.23$ Å, that is, smaller than even the length of the carbon−carbon bond, $d = 1.42$ Å. Here, we use the bending rigidity κ of ≈1.1 eV at room temperature,[19] and Young's modulus $E \approx 22$ eV/Å^2, which is estimated from the elastic modulus of bulk graphite.[20] Therefore, the length l of the observed unsupported graphene beam is ≈10^6 times larger than its effective thickness. One could visualize this geometry as a sheet of paper that extends 100 m without a support. Even though such extraordinary rigidity seems counterintuitive, it is in good agreement with the elasticity theory as shown below.

Each carbon atom in the graphene lattice occupies an area $S_0 = [(3\sqrt{3})/4]d^2$, and graphene's density is given by $\rho = M/S_0 \cong 7.6 \times 10^{-7}$ kg m^{-2}, where M is the mass of a carbon atom. Let us first consider the simplest case of a horizontal rectangular sheet of width w and length l that is infinitely

thin, anchored by its short side (y axis) and free to bend under gravity g. The total energy of the sheet is given by

$$\Sigma = \frac{\kappa}{2} w \int_0^l \mathrm{d}x \left(\frac{d^2h}{dx^2}\right)^2 - \rho g w \int_0^l \mathrm{d}x h \quad (1)$$

where x is the distance from the anchor point at $x = 0$, and $h(x)$ is the deviation from the horizontal axis which is uniform along y. The solution that minimizes the energy and satisfies the boundary conditions is (cf. ref 18)

$$h(x) = \frac{\gamma l^2 x^2}{4} - \frac{\gamma l x^3}{6} + \frac{\gamma x^4}{24} \quad (2)$$

where $\gamma = \rho g/\kappa \approx 0.5 \times 10^{14}$ m^{-3} and $g\rho \cong 7.48 \times 10^{-6}$ N m^{-2}. This yields the maximum bending angle $(\mathrm{d}h/\mathrm{d}x)_{x=l} = \gamma l^3/6$ and, for the membrane in Figure 4 ($l \approx 20\ \mu$m), implies bending angles of several degrees.

The above expression is a gross overestimate for bending of real graphene beams with $w \approx l$ because the discussed purely one-dimensional case takes into account only the bending rigidity and neglects in-plane stresses that inevitably appear in a nonrectangular geometry in order to satisfy boundary conditions.[18] Indeed, sheets of an arbitrary shape should generally experience two-dimensional deformations $h = h(x, y)$, and in the case of graphene, bending becomes limited by the extremely high in-plane stiffness described by E. This makes graphene beams much harder to bend because their apparent rigidity becomes determined by stretching rather than simple bending. Elasticity theory provides an estimate for the typical out-of-plane deformation $\bar{h}$ as (see chapter 14 in ref 18)

$$\frac{\bar{h}}{l} \approx \left(\frac{\rho g l}{E}\right)^{1/3} \approx (3 \times 10^{-14} l)^{1/3} \quad (3)$$

where $l \approx w$ is expressed in micrometers. This means that the gravity induced bending is only of the order of 10^{-4} for graphene slivers such as that shown in Figure 4. We can also estimate the corresponding in-plain strain as $(\bar{h}/l)^2 \approx 10^{-8}$. Note that the crystal also supports an additional weight of many crystalline Cu nanoparticles. We have estimated their average weight density as being 1000 times larger than that of graphene itself. This should result in 100 times larger strain but still of only 10^{-6}. Graphene is known[21] to sustain strain of up to 10% without plastic deformations, albeit edge defects can reduce the limit significantly allowing for the local generation of defects. Still, for the membrane in Figure 4 to collapse, it would require an acceleration of the order of $10^6 g$. This shows that one-atom-thick graphene crystals of a nearly macroscopic size have sufficient rigidity to support not only their own weight but significant extra loads and survive accidental shocks during handling and transportation.

In addition to their intrinsic stiffness, graphene crystals are often corrugated, which further increases their effective thickness and rigidity. Microscopic corrugations (ripples) were previously reported for suspended graphene.[5,8] Some (but not all) of our membranes also exhibited macroscopic corrugations, which extended over distances of many micrometers and were probably induced by accidental bending of the supporting grid or mechanical strain during microfabrication. Similar to the case of corrugated paper, the observed corrugations of graphene should increase its effective rigidity by a factor $(H/a)^2$ where H is the characteristic height of corrugations.[22,23] The increase due to ripples is minor but can be dramatic in the case of large-scale corrugations.

Finally, we note that the described technique for making large graphene membranes can also be applied to many other two-dimensional crystals[3] and ultrathin films, including those materials that cannot withstand aggressive media (e.g., dichalcogenides). One can also use the technique in the case of graphene grown epitaxially on metallic substrates[24,25] in order to either make membranes or study and characterize the epitaxial material further. In this case, the final step in Figure 2 can be substituted by etching away the substrate or peeling off the electrodeposited TEM grid.

In conclusion, we have demonstrated a technique for producing large graphene membranes in a comparatively robust and integratable format. These membranes present a qualitatively new kind of sample support for TEM studies. More generally, large scale suspended graphene samples should allow a wider range of characterization techniques to be employed and will facilitate the incorporation of graphene in various microelectronic, optical, thermal, or mechanical devices. This is a key enabling step for both the investigation and the technological development of this exciting new material. The observed counter-intuitively high rigidity of graphene should change our perception of this one-atom-thick material as fragile and mechanically unstable. It already allows us to understand the previously unexplained fact that graphene does not scroll[12,13] and can be deposited as flat crystals even after being dispersed in a liquid.[2]

Acknowledgment. We thank the Engineering and Physical Sciences Research Council (U.K.) and the Royal Society.

References

(1) Geim, A. K.; Novoselov, K. S. *Nat. Mater.* **2007**, *6*, 183.
(2) Novoselov, K. S.; Geim, A. K.; Morozov, S. V.; Jiang, D.; Zhang, Y.; Dubonos, S. V.; Grigorieva, I. V.; Firsov, A. A. *Science* **2004**, *306*, 666.
(3) Novoselov, K. S.; Jiang, D.; Schedin, F.; Booth, T. J.; Khotkevich, V. V.; Morozov, S. V.; Geim, A. K. *Proc. Natl. Acad. Sci.* **2005**, *102*, 10451–10453.
(4) Zhang, Y.; Tan, Y. W.; Stormer, H. L.; Kim, P. *Nature* **2005**, *438*, 201.
(5) Meyer, J.; Geim, A. K.; Katsnelson, M. I.; Novoselov, K. S.; Booth, T. J.; Roth, S. *Nature* **2007**, *446*, 60.
(6) Bunch, J. S.; van der Zande, A. M.; Verbridge, S. S.; Frank, I. W.; Tanenbaum, D. M.; Parpia, J. M.; Craighead, H. G.; McEuen, P. L. *Science* **2007**, *315*, 490.
(7) Meyer, J.; Girit, C.; Crommie, M.; Zettl, A. *Appl. Phys. Lett.* **2008**, *92*, 123110.
(8) Meyer, J.; Geim, A.; Katsnelson, M.; Novoselov, K.; Obergfell, D.; Roth, S.; Girit, C.; Zettl, A. *Solid State Commun.* **2007**, *143*, 101–109.
(9) Poot, M.; van der Zant, H. S. J. *Appl. Phys. Lett.* **2008**, *92*, 123110.
(10) Balandin, A. A.; Ghosh, S.; Bao, W.; Calizo, I.; Teweldebrhan, D.; Miao, F.; Lau, C. N. *Nano Lett.* **2008**, *8*, 902–907.
(11) Stankovich, S.; Dikin, D. A.; Dommett, G. H. B.; Kohlhaas, K. M.; Zimney, E. J; Stach, E. A; Piner, R. D.; Nguyen, S. T.; Ruoff, R. S. *Nature* **2006**, *442*, 282–286.
(12) Shioyama, H. *J. Mater. Sci. Lett.* **2001**, *20*, 499.
(13) Viculis, L.; Mack, J.; Kaner, R. *Science* **2003**, *299*, 1361.

(14) Blake, P.; Hill, E. W.; Castro Neto, A. H.; Novoselov, K. S.; Jiang, D.; Yang, R.; Booth, T. J.; Geim, A. K. *Appl. Phys. Lett.* **2007**, *91*, 063124.
(15) Bodas, D. S.; Gangal, S. A. *J. Appl. Polym. Sci.* **2006**, *102*, 2094.
(16) Nair, R. R.; Blake, P.; Grigorenko, A. N.; Novoselov, K. S.; Booth, T. J.; Stauber, T.; Peres, N. M. R.; Geim, A. K. *Science* **2008**, *320*, 1308.
(17) Ishigami, M.; Chen, J.; Cullen, W.; Fuhrer, M.; Williams, E. *Nano Lett.* **2007**, *7*, 1643–1648.
(18) Landau, L. D.; Lifshitz, E. M. *Theory of Elasticity*; Pergamon Press: Elmsford, NY, 1986.
(19) Fasolino, A.; Los, J. H.; Katsnelson, M. I. *Nat. Mater.* **2007**, *6*, 858–861.
(20) Blakslee, O. L.; Proctor, D. G.; Seldin, E. J.; Spence, G. B.; Weng, T. *J. Appl. Phys.* **1970**, *41*, 3373–3382.
(21) Walters, D. A.; Ericson, L. M.; Casavant, M. J.; Liu, J.; Colbert, D. T.; Smith, K. A.; Smalley, R. E. *Appl. Phys. Lett.* **1999**, *74*, 3803–3805.
(22) Briassoulis, D. *Computers and Structures* **1986**, *23*, 129–138.
(23) Peng, L. X.; Liew, K. M.; Kitipornchai, S. *Int. J. Mech. Sci.* **2007**, *49*, 364–378.
(24) Coraux, J.; N'Diaye, A.; Busse, C.; Michely, T. *Nano Lett.* **2008**, *8*, 565–570.
(25) de Parga, A. L. V.; Calleja, F.; Borca, B.; M, C. G. Passeggi, J.; Hinarejos, J. J.; Guinea, F.; Miranda, R. *Phys. Rev. Lett.* **2008**, *100*, 056807.

NL801412Y